Catalysis Today 157 (2010) 177–182

Contents lists available at ScienceDirect

Catalysis Today

journal homepage: www.elsevier.com/locate/cattod

Methane oxidation by lattice oxygen of Ni/$BaTi_{1-x}In_xO_{3-\delta}$ catalysts

Verónica García [a,b], Maria Teresa Caldes [b,*], Olivier Joubert [b], Eric Gautron [b], Fanor Mondragón [a], Andrés Moreno [a,*]

[a] *Institute of Chemistry, University of Antioquia, A.A. 1226, Medellín, Colombia*
[b] *Institut des Matériaux Jean Rouxel (IMN), Université de Nantes, CNRS, 2, rue de la Houssinière, BP 32229, 44322 Nantes Cedex 3, France*

ARTICLE INFO

Article history:
Available online 1 March 2010

Keywords:
Perovskite
SOFC
Methane
Partial oxidation
Pulses

ABSTRACT

$BaTi_{1-x}In_xO_{3-\delta}$ perovskites (called BIT*x*) were evaluated as supports of nickel catalysts for methane oxidation in the absence of gas-phase oxygen. Ni/$BaTi_{1-x}In_xO_{3-\delta}$ ($x = 0$ and 0.3) catalysts were studied, by temperature programmed surface reaction of methane (TPSR-CH_4) and pulses at 850 °C. In these conditions, the only oxygen source is the oxide bulk support. TPSR-CH_4 results suggest that the support is able to oxidize the methane producing H_2 and CO at temperatures above 750 °C. Ni/BT and Ni/BIT0.7 catalysts, showed a high selectivity towards partial oxidation products. Ni/BIT0.7 catalyst was more stable than Ni/BT due to the existence of Ni–In alloys which catalyze less the cracking reaction. Moreover, the higher ionic conductivity of BIT0.7 facilitates the O^{2-} ions diffusion to the surface and promotes the oxidation of carbonaceous deposits formed on the metal–support interface preventing thus catalyst deactivation.

1. Introduction

$BaTi_{1-x}In_xO_{3-\delta}$ ($0 \leq x \leq 0.7$) perovskites, called BIT*x*, have been studied as electrolytes for solid oxide fuel cells operating directly with natural gas [1]. $BaTi_{0.7}In_{0.3}O_{3-\delta}$ (BIT0.7) can also be used as cermet anode when it is associated to 30 wt% of Ni [2]. The high ionic conductivity of BITx compounds ($\sim 10^{-2}$ S/cm at 700 °C for $0.2 \leq x \leq 0.7$) suggests a good diffusion of ions O^{2-} through the support, which is essential for the oxidation of coke formed at the Ni-support interface during hydrocarbons reforming. Several authors have reported that the presence of oxygen vacancies in the support, associated with a certain level of ionic (O^{2-}) and/or electronic conductivity, favors the oxidation of the coke formed during methane conversion avoiding the deactivation of the catalyst [3–6]. In fact 30 wt% Ni/BIT07 anodes exhibit a good resistance to coking under particular operating conditions [7]. In order to better understand the influence of the BIT*x*-type phases on the catalytic activity of the cermets, a low Ni content (5 wt%) was deliberated chosen to enhance the BIT*x* contribution. Recently, we found that 5 wt% Ni/$BaTi_{1-x}In_xO_{3-\delta}$ compounds have interesting properties as CO_2 methane reforming catalysts, especially Ni/$BaTi_{0.7}In_{0.3}O_{2.85}$ (Ni/BIT0.7) catalyst which exhibits a considerable stability and a low coke-deposition [8]. However, the interactions between CH_4 and Ni/$BaTi_{1-x}In_xO_{3-\delta}$ were not investigated. The main purpose of this work is to investigate the influence of the oxygen ion mobility of the support, on the CO/CO_2 selectivity and coking phenomena during CH_4 oxidation. For this purpose, temperature programmed surface reaction of methane (TPSR-CH_4) and pulse experiences in the absence of gas-phase oxygen were performed. This replicates the SOFC environment, in which oxidation occurs through oxygen ions.

2. Experimental

$BaTiO_3$ (BT) and $BaTi_{0.7}In_{0.3}O_{2.85}$ (BIT0.7) powders were prepared by solid state reaction, mixing In_2O_3, TiO_2 and $BaCO_3$. These reagents were mixed in a mortar with acetone and the dried mixture was calcinated at 1200 °C for 24 h in air. Finally, powders were uniaxially pressed into pellets and sintered in air at 1350 °C for 24 h. In order to reduce the size of the particles, the pellets were ground in a planetary ball mill device for 2 h at 500 rpm, and the powders obtained were sieved through a 140 mesh screen. To prepare NiO/$BaTi_{1-x}In_xO_{3-\delta}$ catalyst precursors, $BaTi_{1-x}In_xO_{3-\delta}$ powders were impregnated with aqueous nickel nitrate solution (5 wt% Ni). The obtained paste was dried at room temperature, and then calcined at 750 °C in air for 3 h.

X-ray diffraction (XRD) patterns of the supports and catalysts were recorded with a Bruker D8 diffractometer using Kα radiation of Cu. Structure refinements were carried out using the program FULLPROF [9]. Electrical conductivity measurements of supports were made by impedance spectroscopy using dense pellets. A model 1260 high frequency response analyzer of M/s Solartron

---

* Corresponding authors.
E-mail addresses: maite.caldes@cnrs-imn.fr (M.T. Caldes), jamoreno@matematicas.udea.edu.co (A. Moreno).

0920-5861/$ – see front matter © 2010 Elsevier B.V. All rights reserved.
doi:10.1016/j.cattod.2010.01.021

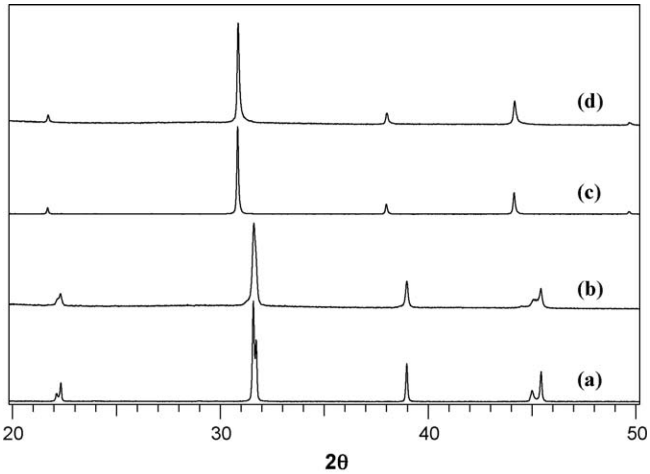

Fig. 1. X-ray diffraction patterns of (a) BT, (b) Ni/BT, (c) BIT0.7, (d) Ni/BIT0.7.

(Schlumberger, UK) with a 500 mV of ac perturbation was used from 1 Hz to 2 MHz, between 300 and 800 °C, in air. Both sides of the pellets were coated with gold electrodes. BET surface area was measured on a Micromeritics ASAP 2010 M apparatus employing N_2 physisorption at −196 °C using multipoint BET method. Transmission electron microscopy was carried out on a microscope Hitachi H9000NAR operating at 300 kV, equipped with an energy dispersive X-ray (EDX) analyzer. Temperature programmed surface reaction of methane (TPSR-CH_4) was carried out using 50 mg of catalyst, held on quartz wool in a vertical quartz tube. The gases feed were passed through oxygen filter to eliminate trace amounts of oxygen. The tests were carried out over reduced catalyst at 700 °C for 1 h in 40 ml/min of pure hydrogen, and then the temperature was decreased to room temperature. The temperature programmed surface reaction was performed with 50 ml/min mixture of CH_4/Ar (4% CH_4) at a rate of 10 °C/min to 850 °C and held for 1 h under the mixture reaction. The reactor effluent was online analyzed using a mass spectrometer (Pfeiffer Vacuum, Omnistar GSD 301). Carbon deposition was determined by temperature programmed oxidation (TPO) in the temperature range 50–850 °C at a total flow rate of 50 ml/min (10% O_2/Ar). Pulse experiments were carried out using a reactor system similar to that of TPSR-CH_4 experiments. First, 50 mg of powder was placed in a quartz tube and heated to 700 °C in hydrogen flow for 1 h then the gas composition was changed to argon to remove hydrogen before pulse experiments. The sample was subsequently heated to 850 °C in argon. Then the sample was exposed to 10 pulses of 1 ml of methane, separated by 10-min intervals of 33 ml/min Ar. Well-defined and repeatable pulses were obtained by using a 6-ways switching valve. The reactor effluent was continually analyzed with a mass spectrometer (Pfeiffer Vacuum Omnistar GSD301).

3. Results

3.1. Characterization

The experimental XRD patterns of $BaTiO_3$ (BT) and $BaTi_{0.7}In_{0.3}O_{2.85}$ (BIT0.7) are shown in Fig. 1. Both compounds are single-phase and exhibit a perovskite-type structure. However, whiles BT can be described in the tetragonal space group *P*4*mm*, BIT07 exhibits a cubic perovskite structure with a space group *Pm*-3*m*. The cell parameters are summarized in Table 1. Surface areas of the catalyst precursors and the electrical conductivity of the supports at 700 °C (σ_{700}) are also shown in Table 1. The conductivity values measured are in good agreement with those already published [1]. The electrical conductivity of these compounds is mainly anionic. $BaTi_{0.7}In_{0.3}O_{2.85}$ exhibits a higher ionic conductivity at 700 °C because it contains a number of charge carriers (oxygen vacancies) larger than that of $BaTiO_3$. Specific surface areas of the catalyst precursors are 3.5 m^2/g. These low values are not surprising due to the high calcination temperature required to synthesize these compounds.

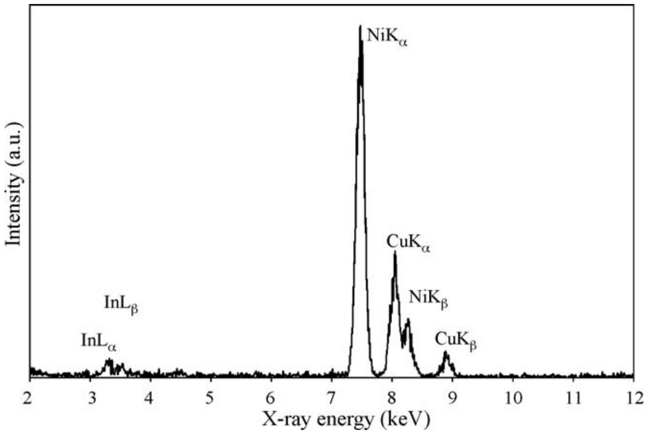

Fig. 2. EDX spectrum of metallic particle supported by BIT0.7 (Cu signal from copper grid).

To prepare $Ni/BaTi_{1-x}In_xO_{3-\delta}$ catalysts, $NiO/BaTi_{1-x}In_xO_{3-\delta}$ precursors were reduced under pure hydrogen for 1 h. Corresponding XRD patterns are shown in Fig. 1. After reduction process no impurity was observed. However, for Ni/BIT0.7 a broadening of the diffraction peaks of the support is observed.

In order to get insight into the microstructure and chemical composition, a transmission electron microscopy (TEM) study and EDX microprobe analyses were carried out over the $Ni/BaTi_{1-x}In_xO_{3-\delta}$ catalysts. Numerous metallic particles distributed over the support surface are observed in both catalysts. The metallic particle size was determined by counting only spherically shaped particles. A total of 100 particles were analyzed from the micrographs of the Ni/BT and Ni/BIT0.7 catalysts. The average surface diameter of the metallic particles given by $\langle d\rangle = \sum n_i d_i^3 / \sum n_i d_i^2$ expression [10] was 47 and 37 nm for the Ni/BT and Ni/BIT0.7 respectively. The minor difference observed in particle size indicates that the dispersion of Ni particles must be quite similar in both catalysts.

Chemical composition of the metallic particles was studied by EDX. In the case of Ni/BT all the particles observed were exclusively composed of Ni. However, for Ni/BIT0.7 catalyst, indium was also detected into some Ni particles. In Fig. 2 a characteristic EDX spectrum of Ni–In particles is shown. These results suggest that under reducing atmosphere, a small amount of In^{3+} of the support can be reduced to In^0 which reacts with Ni to form a Ni–In alloy.

Table 1
Physical properties of the supports and BET surface areas of $NiO/BaTi_{1-x}In_xO_{3-\delta}$ precursor catalysts.

Catalyst	Symbol	*a* cell parameter (Å) of the support	Electrical conductivity of the support at 700 °C (S/cm)	BET surface area (m^2/g)
$Ni/BaTiO_3$	Ni/BT	3.9912(4)	4×10^{-4}	3.2
$Ni/BaTi_{0.7}In_{0.3}O_{2.85}$	Ni/BIT0.7	4.0973(5)	1×10^{-2}	3.5

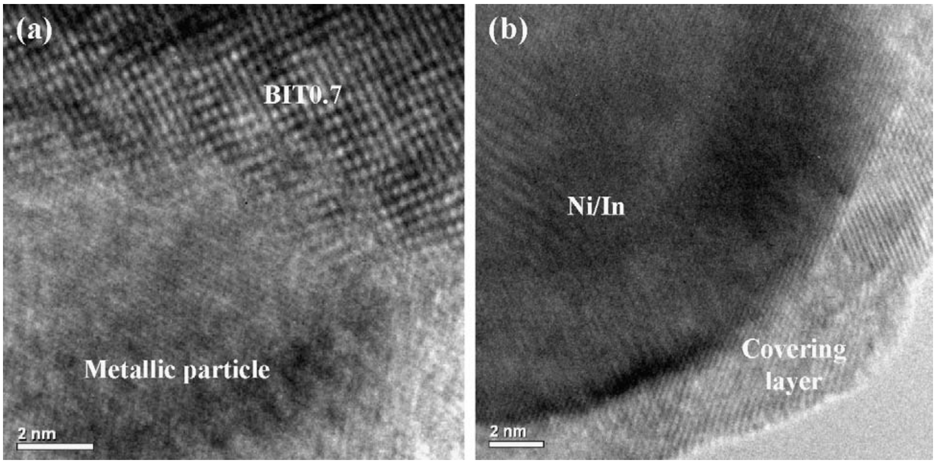

Fig. 3. HREM micrographs of Ni/BIT0.7 catalyst.

The In exsolution should induce structural defects in the support which could explain the broadening of the diffraction peaks observed. In Fig. 3a, a high resolution electron microscopy (HREM) image of an In–Ni particle supported on a BIT0.7 crystal is shown. The contrast observed far from the Ni(In)–BIT0.7 interface is typical of a perovskite-type structure; for this defocus value the BO_2 layers appear as right lines of white spots. However, near from the metallic particle, the contrast of the BO_2 layers is significantly perturbed, possibly due to the exsolution of indium. Moreover, as shown in Fig. 3b, some Ni–In particles are covered and/or supported by a thin layer whose chemical composition could not been determined. Further TEM experiments are in progress to better characterize both structural defects and the nature of this layer.

The indium segregation should be also accompanied by a modification of the chemical composition of the support. The (Ba + Ti)/In ratios for BIT07 and the Ni/BIT07 catalyst were obtained by EDX. Nanometric probes were used to isolate zones of the support without metallic particles. For Ni/BIT0.7 catalyst, experimental ratio is higher (7.7) than theoretical one (6.1) which reflects the existence of In-poor zones. The detection limit of the EDX technique is 5–10% molar. It should be noted that a sublimation of In^0 cannot be excluded.

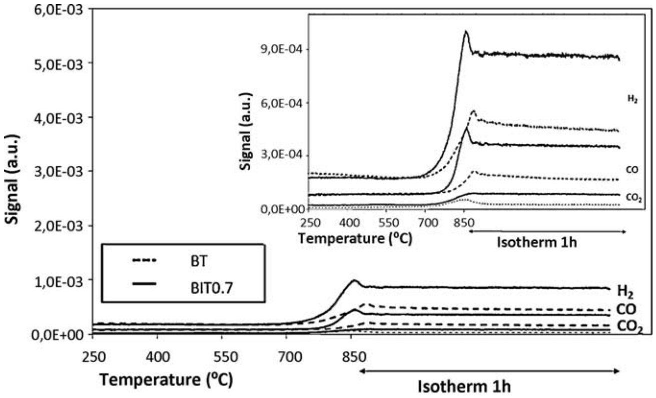

Fig. 4. MS signals of H_2, CO, CO_2 detected during TPSR-CH_4 of supports.

3.2. Catalytic activity

The results from TPSR-CH_4 for BT and BIT0.7 supports are presented in Fig. 4. The reactants and products were detected by a mass spectrometer using m/e = 2 (H_2), 15 (CH_4), 18 (H_2O), 28 (CO), 32 (O_2) and 44 (CO_2). The 15, 18 and 32 signals are not shown in the figure to improve clarity. As observed in the insert of Fig. 4, the CO_2 formation started at 740 °C and reached the maximum at 840 °C for both oxides. However, the major products detected were CO and H_2. This result suggests that the oxygen surface species got consumed producing CO_2 at the early stage of oxidation reaction, whereas from 780 to 850 °C the reaction becomes more selective toward partial oxidation products. Van den Bossche and McIntosh [11] observed the same trend as $La_{0.75}Sr_{0.25}Cr_xMn_{1-x}O_{3-\delta}$ favoring total oxidation at low temperature ($T < 600\,°C$) and partial

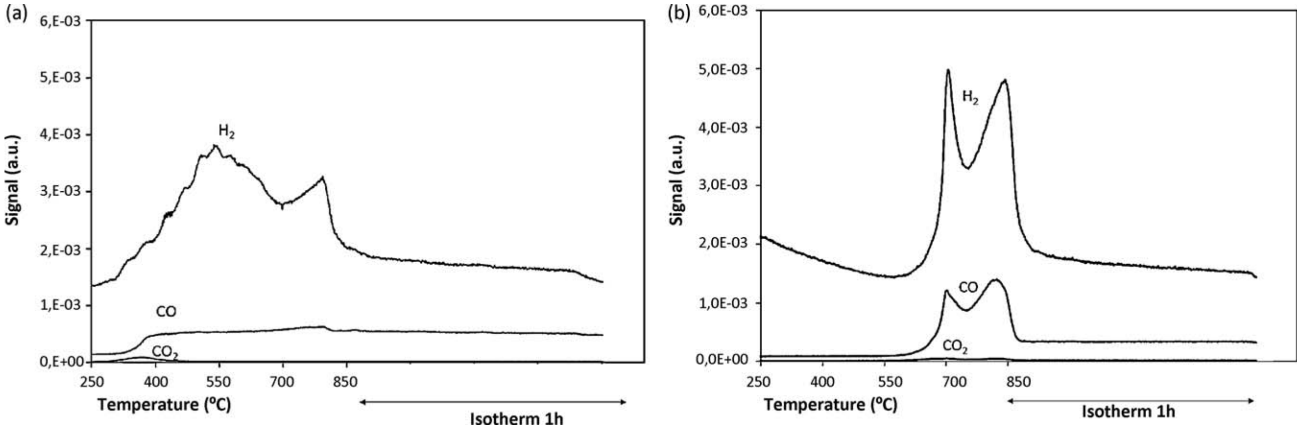

Fig. 5. MS signals of H_2, CO, CO_2 detected during TPSR-CH_4 over (a) Ni/BT and (b) Ni/BIT0.7.

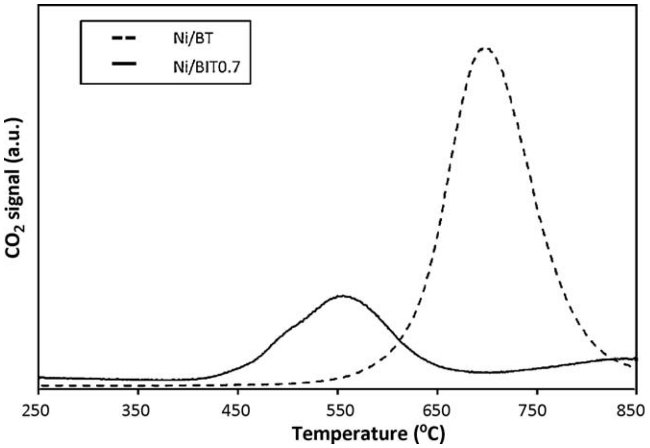

Fig. 6. TPO of Ni/BT and Ni/BIT0.7 after TPSR-CH_4.

oxidation at higher temperature. Qualitatively, the activity of BIT0.7 support is higher than that of BT, which is probably related to the higher reducibility of In^{3+} with respect to Ti^{4+} and to the higher anionic conductivity of BIT0.7. As shown in Fig. 4, an increase of CO formation is observed with temperature. Moreover, during the isothermal a constant production is detected. In fact, the CO formation depends on the availability of the oxygen species which is related to the oxygen ions mobility that increases with temperature [12,13]. Furthermore, the constant CO production suggests that formation rate at 850 °C is quite low.

TPSR-CH_4 profiles for Ni/BT and Ni/BIT0.7 catalysts are shown in Fig. 5. As in the case of supports, partial oxidation products H_2 and CO were predominant, with a minor formation of CO_2. However, the catalytic activity of catalysts is largely highest. Moreover, while the reactivity of the supports is similar to each other that of catalysts is quite different. For Ni/BT catalyst, H_2 profile showed a broad peak centered at 550 °C (plugged reactor) and the CO signal is relatively low. However, in the case of Ni/BIT0.7 H_2 and CO formation is characterized by two peaks, which are centered at 700 and 850 °C. H_2 and CO production started at 600, 300 °C upper than that observed for catalyst of Ni/BT, suggesting a strong metal–support interaction (SMSI) effect, as will be discussed later.

Both catalysts exhibit quite similar H_2 and CO profiles, but the amount of CO formed is less important. Finally, the decreasing of hydrogen and CO formation observed during the isothermal period is attributed to the depletion of bulk lattice oxygen and coke deposition.

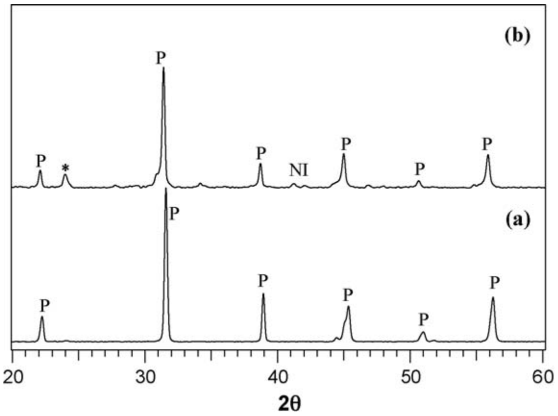

Fig. 8. X-ray diffraction patterns of used catalysts (a) Ni/BT and (b) Ni/BIT0.7. P (perovskite), NI (Ni/In alloy), (*) impurity.

After TPSR-CH_4 experiments, spent catalysts were reoxidized (TPO) while measuring the CO_2 (m/e = 44) release. The amount of CO_2 produced was related to the amount of carbon deposited on the sample during TPSR-CH_4 experiment. According to the TPO profiles shown in Fig. 6, only one CO_2 peak was observed. The peak of CO_2 formation was detected at 550 °C for Ni/BIT0.7 while for Ni/BT it was observed at 700 °C suggesting that carbon type is not the same in each catalyst. Thus, the peak at 500 °C may be attributed to oxidation of carbide-like nickel species [14] and the peak at 700 °C could be ascribed to the oxidation of carbon filaments [15]. As shown in Fig. 7a, a very thin layer of graphite (∼2 nm) encapsulates Ni–In particles of the Ni/BIT0.7 catalyst. However, for Ni/BT catalyst carbon fibers are also observed (see Fig. 7b). Additionally, it must be noted that the amount of carbon deposited on the Ni/BT catalyst is noticeably larger.

XRD patterns of spent catalysts are presented in Fig. 8. The patterns for as-prepared and spent Ni/BT catalysts are quite similar and no additional phases could be detected. Nevertheless a broadening of the diffraction peaks is observed after TPSR-CH_4 experiment. In the case of Ni/BIT0.7 this broadening is accompanied by two new peaks of low intensity which can be assigned to Ni/In alloys (δ-In_3Ni_2, JCPDF # 00-007-0298).

In order to look further into the catalytic behaviour of these compounds and to quantify the major oxidation products, experiments in which methane was pulsed over the sample at constant temperature 850 °C were performed. The conversion data obtained from CH_4-pulse reaction over Ni/BT and Ni/BIT0.7 are

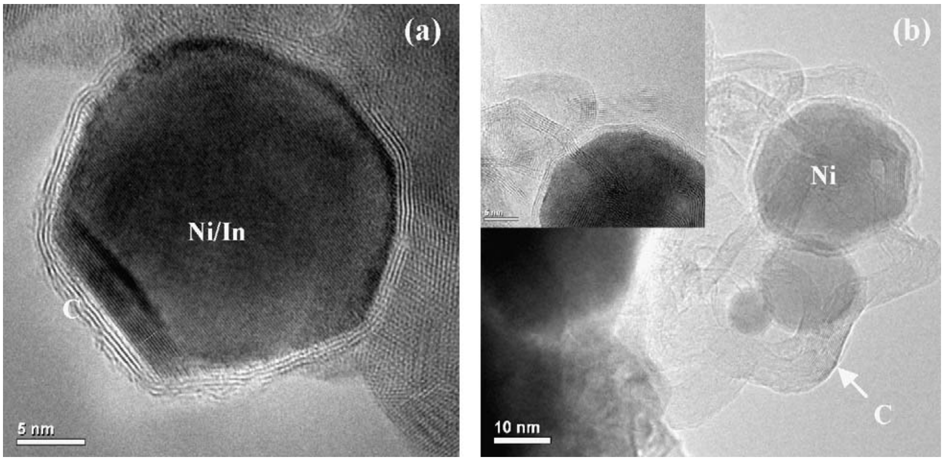

Fig. 7. TEM micrographs of Ni/BT (a) and Ni/BIT0.7 (b) used catalyst.

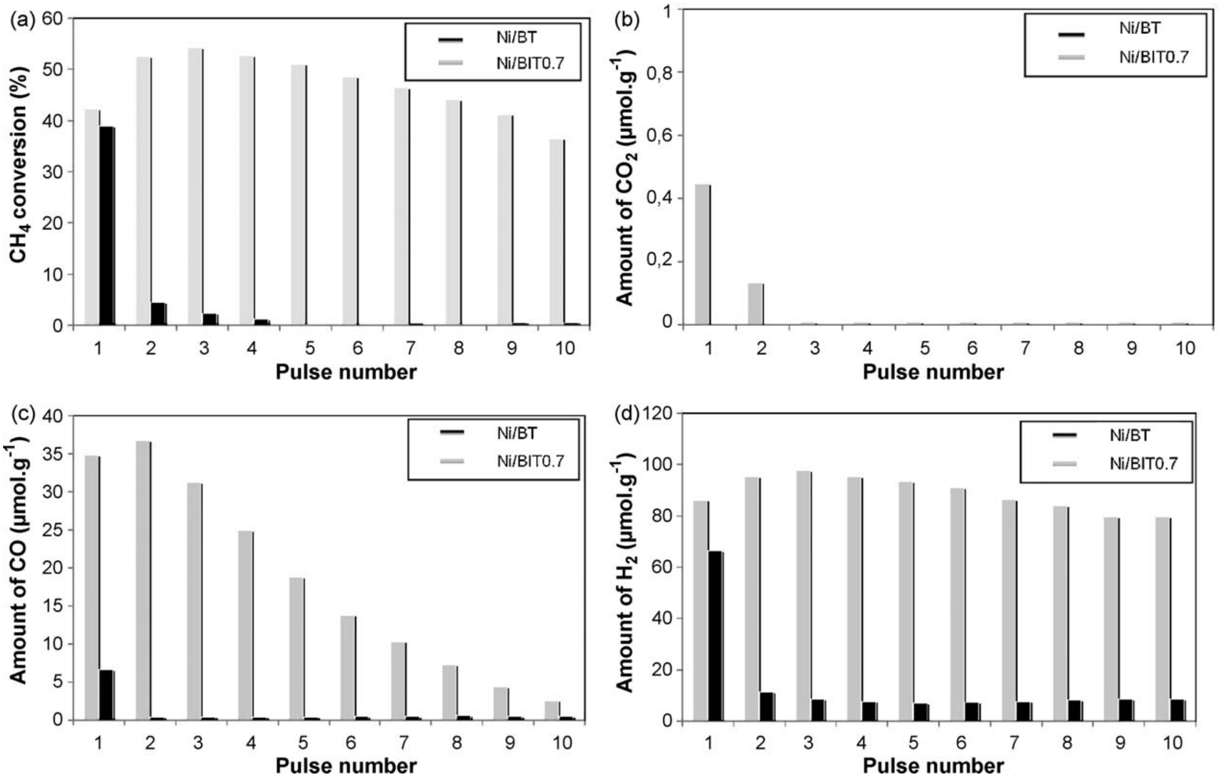

Fig. 9. Methane conversion (a), amount of CO_2 (b), CO (c) and H_2 (d) formed during CH_4 pulses on Ni/BT and Ni/BIT0.7.

depicted in Fig. 9a. Methane conversion is relatively high for both catalysts but the Ni/BT catalyst was only active at the initial stage. After four pulses the reactor was plugged indicating an abrupt coke formation which obstructs the active sites. In the case of Ni/BIT0.7 catalyst, methane conversion increases slightly during the first three pulses, suggesting that reducible species still subsist even after a pre-treatment under H_2 at 700 °C. A modification of the thin layer surrounding metallic particles described above could also explain this feature. Between the third and tenth pulse the methane conversion decreases from 50% to 37%.

CO, CO_2 and H_2 production over Ni/BIT0.7 catalyst are shown in Fig. 9. Selectivity toward partial oxidation products is evidenced under isothermal (850 °C) and dynamic reaction (TPSR-CH_4). CO, CO_2 and H_2 yield decreases during the methane pulses; similar results have been recently reported by Yan et al. [16] for 8% Ni/TiO_2 catalyst. A very low CO_2 formation was only observed during the first CH_4 pulse. These results indicate that the catalysts reactivity is a function of the oxygen availability but the selectivity is not modified during the pulses, as shown in Fig. 9.

The amount of oxygen involved in the pulse reaction cannot be only ascribed to surface oxygen due to the low surface area (3.5 m^2/g). Thus, the bulk oxygen also participates to methane oxidation thanks to O^{2-} migration into perovskite lattice [11]. For the partial oxidation reaction, the expected H_2/CO ratio is equal to 2 as it was observed for the first pulse, however from the second pulse the H_2/CO ratio was always above 2 suggesting that methane decomposition reaction also occurs.

4. Discussion

TPSR-CH_4 measurements in absence of oxygen showed that over BT and BIT0.7 supports, the methane is selectively oxidized to H_2 and CO by oxygen lattice above 780 °C. The activity of BIT0.7 support is higher than that of BT, which is related to the higher reducibility of In^{3+} with respect to Ti^{4+}, and to the higher anionic conductivity of BIT0.7.

Methane oxidation over BT and BIT0.7 follows a Mars–Van Krevelen mechanism, where the oxidation activity is dictated by B-site cation [17,18]. Surface oxygen species react with methane generating oxygen vacancies which are replenished by oxygen diffusion from the bulk, becoming available for methane oxidation. The charge balance is maintained by B-site of the perovskite [19,20].

Ni/BIT*x* catalysts showed a higher activity and selectivity towards the partial oxidation of methane than the supports even at lower temperatures. Nevertheless, it must be noted that metallic particles also favor methane decomposition. Even if at initial stage of methane oxidation Ni/BT and Ni/BIT0.7 exhibit similar activity, a highest stability is found for Ni/BIT0.7 catalyst. This feature is due to a synergy between two factors, the existence of Ni–In alloy particles and the ability of support to oxidize the coke thanks to O^{2-} mobility. Ni–In alloy formation and the thin layer covering metallic particles observed by HREM indicate a strong metal-support interaction (SMSI) effect. In fact, in the literature has been reported that the support can influence the catalytic activity of the metallic phase not only through dispersion but also in other ways [16,19–21]. For instance, Ruckenstein et al. [22–24] reported a partial coverage of rhodium particles by species generated via support reduction in Rh catalysts supported on reducible-oxides. The authors correlate this SMSI effect to the low activity exhibited by these catalysts. In our case the strong interaction between nickel and BIT0.7 is responsible for the high methane activation temperature and the high stability of Ni/BIT0.7 catalyst.

The TPSR-CH_4 and pulses experiments showed that the performance of the supported nickel catalyst is strongly affected by the support. H_2 and CO were the main reaction products, with a minor formation of CO_2. Taking into account that these experiments were performed in the absence of gas-phase oxygen, the CO and CO_2 formation necessarily involves the oxidation of carbon deposits and/or CH_4 by the lattice oxygen of the support [12,25,26]. The first H_2 peak observed in the TPSR-CH_4 at 700 °C over Ni/BIT0.7 could be ascribed to the methane decomposition over the metallic particles according to reaction: $CH_4 \rightarrow C$ (or CH_x) + $2H_2$ while the CO/CO_2 production is related to carbon oxidation: $CH_x + [Ox]_s \rightarrow CO_x + 2H_2$. CO_2 formation could be likely due to the reduction of surface oxygen ($[Ox]_s$) which are the most reactive oxygen species. Moreover, the second H_2/CO peak in TPSR-CH_4 could be related to the direct oxidation of CH_4 or CH_x by bulk oxygen ($[Ox]_b$) via oxygen mobility into the support, according to the reaction $CH_x + [Ox]_b \rightarrow CO + 2H_2$. According to this model, the higher anion conductivity displayed by BIT0.7 could explain the highest activity and stability of the Ni/BIT0.7 catalyst for the direct methane oxidation.

5. Conclusions

$BaTi_{1-x}In_xO_{3-\delta}$ perovskites (called BITx) were evaluated as supports of nickel catalysts for methane oxidation in the absence of gas-phase oxygen. $BaTi_{1-x}In_xO_{3-\delta}$ and Ni/$BaTi_{1-x}In_xO_{3-\delta}$ ($x = 0$ and 0.3) were studied, by temperature programmed surface reaction of methane (TPSR-CH_4) and pulses at 850 °C, only for the catalysts. The reducibility of B cation (ABO_3) and the anionic conductivity of the support strongly influence the catalytic activity and selectivity of the BITx compounds. Ni/BT and Ni/BIT0.7 catalysts showed a high selectivity towards partial oxidation products. Ni/BIT0.7 catalyst was more stable than Ni/BT due to the existence of Ni–In alloys which catalyze less the cracking reaction. Ni/BIT0.7 catalyst can be considered as a suitable material for selective oxidation of methane.

Acknowledgements

The authors thank to the University of Antioquia for financial assistance under the Sostenibilidad program 2009/2010. V. García thanks to the University of Antioquia and Colciencias for the PhD scholarship and to the European Institute for Energy Research for financial support.

References

[1] V. Jayaraman, A. Magrez, M. Caldes, O. Joubert, M. Ganne, Y. Piffard, L. Brohan, Solid State Ionics 170 (2004) 17.
[2] T. Delahaye, O. Joubert, M.T. Caldes, Y. Piffard, P. Stevens, Solid State Ionics 177 (2006) 2945.
[3] M.L. Toebes, J.H. Bitter, A.J. van Dillen, K.P. de Jong, Catal. Today 76 (2002) 33.
[4] H. Hayashi, H. Inaba, M. Matsuyama, N.G. Lan, M. Dokiya, H. Tagawa, Solid State Ionics 122 (1999) 1.
[5] E.A. Lombardo, M.A. Ulla, Res. Chem. Intermed. 24 (5) (1998) 581.
[6] X.P. Dai, Q. Wu, R.J. Li, C.C. Yu, Z.P. Hao, J. Phys. Chem. B 110 (2006) 25856.
[7] F. Moser, M.T. Caldes, O. Joubert, Y. Piffard, V. Garcia, M. Zahid, Proceeding in Fundamentals and Developments of Fuel Cell Conference (FDFC), Nancy, 2008.
[8] V. García, M. Caldes, O. Joubert, A. Moreno, F. Mondragón, C. Batiot-Dupeyrat, in: Proceedings of the XXI SICAT, Malaga-Benalmadena-Costa España, 2008.
[9] J. Rodríguez-Carvajal, Physica B 192 (1993) 55.
[10] D.G. Mustard, C.H. Bartholomew, J. Catal. 67 (1981) 186.
[11] M. van den Bossche, S. McIntosh, J. Catal. 255 (2008) 313.
[12] T.-J. Huang, C.-H. Wang, Catal. Lett. 118 (2007) 103.
[13] X.P. Dai, Ch.Ch. Yu, W. Qiong, Chin. J. Catal. 29 (2008) 954.
[14] H.M. Swaan, V.C.H. Kroll, G.A. Martin, C. Mirodatos, Catal. Today 21 (1994) 571.
[15] C. Pham-Huu, N. Keller, V.V. Roddatis, G. Mestl, R. Schlogl, M.J. Ledoux, Phys. Chem. Chem. Phys. 4 (2002) 514.
[16] A. Yan, B. Liu, Y. Dong, Z. Tian, D. Wang, M. Cheng, Appl. Catal.: Environ. 80 (2008) 24.
[17] N. Yamazoe, Y. Teraoka, Catal. Today 8 (1990) 175.
[18] H.L. Forni, I. Rossetti, Appl. Catal. B: Environ. 38 (2002) 29.
[19] T. Ramos, A. Atkinson, Solid State Ionics 170 (2004) 275.
[20] H.J. Wei, Y. Cao, W.J. Ji, C.T. Au, Catal. Commun. 9 (2008) 2509.
[21] K.J. Boon, F.P.F. van Berkel, E.R. Stobbe, in: Proceedings of the 15th World Hydrogen Energy Conference ECN-RX-05-050, Yokohama, Japan, 2004.
[22] E. Ruckenstein, H.Y. Wang, J. Catal. 187 (1999) 151.
[23] J. Barrault, A. Alouche, V. Paul-Boncour, L. Hilaire, A. Percheron-Guegan, Appl. Catal. 46 (1989) 269.
[24] R. Burch, A.R. Flambard, J. Catal. 78 (1982) 389.
[25] R. Li, Yu Ch, Sh. Chen, J. Natl. Gas Chem. 11 (2002) 137.
[26] V.A. Sadykov, T.G. Kunznetsova, G.M. Alikina, Y.V. Frolova, A.I. Lukashevich, Y.V. Potapova, V.S. Muzykantov, V.A. Rogov, V.V. Kriventsov, D.I. Kochubei, E.M. Moroz, D.I. Zyunzin, V.I. Zaikovskii, V.N. Kolomiichuk, E.A. Paukshitis, E.B. Burgina, V.V. Zyryanov, N.F. Uvarov, S. Neophytides, E. Kemnitz, Catal. Today 93 (2004) 45.